Journal of MASS SPECTROMETRY

MALDI-TOF MASS SPECTROMETRY ANALYSIS OF PROTEINS AND LIPIDS IN ESCHERICHIA COLI EXPOSED TO COPPER IONS AND NANOPARTICLES

Journal:	*Journal of Mass Spectrometry*
Manuscript ID	JMS-16-0061.R1
Wiley - Manuscript type:	Research Article
Date Submitted by the Author:	n/a
Complete List of Authors:	Calvano, CD; University of Bari, Chemistry Department Picca, Rosaria Anna; Università degli Studi di Bari Aldo Moro, Dipartimento di Chimica Bonerba, Elisabetta; Università degli Studi di Bari Aldo Moro, Dipartimento di Medicina Veterinaria Tantillo, Giuseppina; Università degli Studi di Bari Aldo Moro, Dipartimento di Medicina Veterinaria Cioffi, Nicola; Università degli Studi di Bari Aldo Moro, Dipartimento di Chimica Palmisano, Francesco; Università degli Studi Bari Aldo Moro, Dipartimento di Chimica
Keywords:	MALDI, protein, nano-antimicrobials, copper nanoparticle, bacteria, lipid

MALDI-TOF MASS SPECTROMETRY ANALYSIS OF PROTEINS AND LIPIDS IN ESCHERICHIA COLI EXPOSED TO COPPER IONS AND NANOPARTICLES

C.D. Calvano[1,2*], R.A. Picca[1], E. Bonerba[3], G. Tantillo[3], N. Cioffi[1,2*], F. Palmisano[1,2]

[1]*Dipartimento di Chimica and* [2]*Centro di Ricerca Interdipartimentale S.M.A.R.T., Università degli Studi di Bari Aldo Moro, Campus Universitario, Via E. Orabona 4, 70126 Bari (Italy)*

[3]*Dipartimento di Medicina Veterinaria, Università degli Studi di Bari, Strada provinciale per Casamassima Km 3, Valenzano (BA), 70100 Bari (Italy)*

Keywords: MALDI, protein, lipid, bacteria, copper nanoparticle, nano-antimicrobials

** Authors for correspondence, email: cosimadamiana.calvano@uniba.it, nicola.cioffi@uniba.it*

Abstract

Escherichia coli (*E. coli*) is one of the most important foodborne pathogens to the food industry responsible for diseases as bloody diarrhea, hemorrhagic colitis and life-threatening hemolytic-uremic syndrome. For controlling and eliminating *E. coli*, metal nano-antimicrobials (NAMs) are frequently used as bioactive systems for applications in food treatments. Most NAMs provide controlled release of metal ions, eventually slowing down or completely inhibiting the growth of undesired microorganisms. Nonetheless, their antimicrobial action is not totally unraveled and is strongly dependent on metal properties and environmental conditions.

In this work, we propose the use of MALDI TOF mass spectrometry as a powerful tool for direct, time efficient, ~~accurate~~ plausible identification of the cell membrane damage from bacterial strains exposed to copper-based antimicrobial agents, such as soluble salts (chosen as simplified AM material) and copper nanoparticles (CuNPs). *E. coli* ATCC 25922 strain was selected as "training bacterium" to set up some critical experimental parameters (i.e. cell concentration, selection of the MALDI matrix, optimal solvent composition, sample preparation method) for the MS analyses. The resulting procedure was then used to attain both protein and lipid fingerprints from *E. coli* after exposure to different loadings of Cu salts and NPs. Interestingly, bacteria exposed to copper showed over-expression of copper binding proteins and degradation of lipids when treated with soluble salt. These findings were completed with other investigations, such as microbiological experiments.

1. Introduction

Escherichia coli (*E. coli*) is a Gram-negative bacterium that lives in the lower intestine of humans and animals. Most *E. coli* strains are harmless, but some serotypes can cause common infections as life-threatening bloodstream and urinary diseases [1] and food poisoning in their hosts [2]. In particular, enterohemorrhagic *E. coli* (EHEC) O157:H7 is one of the most important foodborne pathogens to the food industry and has resulted in a large number of product recalls due to food contamination [3]. These bacteria can infect food in different ways: contact with intestines of an animal during meat or poultry processing, use of growing or shipping water containing animal or human waste, precarious transport or storage of food, unsafe food handling or preparation. *E. coli* can persist in acidic foods and its infective dose is as low as 10-100 cells [4]. Despite remarkable efforts that have been made on monitoring and reducing *E. coli* from foods, associated foodborne illnesses continued to increase in last years. Further, their antibiotic resistance rates are fast rising, especially with regard to fluoroquinolones and cephalosporins triggering the occurrence of multidrug-resistant strains [5]. A valid alternative to antibiotics can be represented by metal nano-antimicrobials (NAMs) used as bioactive systems with selective toxicity to bacteria and low human and environmental toxicity [6]. Indeed, most NAMs provide controlled release of metal ions, eventually slowing down or completely inhibiting the growth of undesired microorganisms [7]. To this purpose, various NAMs based on silver, zinc oxide, iron oxide, titanium dioxide, copper and copper oxide have been developed for applications in food and textile industries, biomedicine, and other fields [8, 9]. Among them, soluble copper compounds and copper alloys have been shown to provide excellent antimicrobial activity against bacterial, fungal, and viral pathogens [10-12]. Previous studies have suggested that reactive oxygen species (ROS), radical by-products of aerobic respiration, are a central part of the killing mechanism upon exposure to soluble copper which can directly cause irreparable damage such as the oxidation of proteins, cleavage of DNA and RNA

molecules, and membrane damage due to lipid peroxidation [13-16]. However, few papers have been issued so far about the antibacterial properties of nano-sized scale copper materials [17, 18]. To date, the modes of action of NAMs are not well understood since they depend on many factors as particles physicochemical properties including size, shape, chemical modification and coating, target bacteria, physiological state of the bacteria, environmental conditions, and so on. For instance, the damage to DNA induced by hydrogen peroxide and reduced copper is well documented in eukaryotic cells but is not confirmed in yeasts and *E. coli* [19] so is strictly dependent from the genetics, cell wall structure, and metabolic pathways of target microorganisms. Many papers deal with the valuation of the nano-antimicrobial activity against *E. coli* by usually employing conventional microbial protocols as disc diffusion test, determination of minimum inhibitory concentrations (MIC) and minimum bactericidal concentration (MBC) [20,21]. In these tests, the lowest concentration of AM inhibiting the growth or killing the microorganism is assessed but no information about the mechanism of contact-mediated killing by copper can be inferred. Recently, Honh *et al.* [22] found, by indirectly monitoring the production of malondialdehyde by-product using TBARS (thiobarbituric acid-reactive substances) assay kit, that the copper killing activity is mediated by the ROS-catalyzed nonenzymatic peroxidation of membrane lipids; nevertheless any examination on the membrane lipids modification was carried out. A careful study, at the molecular level, to monitor the real time changes of microorganisms as a response to various NAM exposures, would help in rationalizing the mechanism behind the copper mediated inactivation. To this aim, the present work focuses on obtaining protein and lipid profiles of cell membranes from bacterial strains treated with copper antimicrobial agents, such as soluble salts (chosen as reference) and in house synthetized copper nanoparticles (CuNPs) by using a mass spectrometry (MS) technique. Among MS techniques, matrix-assisted laser desorption ionization time-of-flight (MALDI-TOF) has shown its ability in providing useful information for

microorganisms identification and differentiation, typically through peptide/protein fingerprinting, due to its speed and sensitivity that allow rapid analyses with minimal sample preparation [23–25]. Indeed, two commercial MALDI-TOF MS systems are today available for microbial identification: the Bruker MALDI Biotyper (Bruker Daltonics, Billerica, MA) and the bioMe´rieux VITEK MS (bioMe´rieux, Durham, NC). Highly abundant proteins with characteristic patterns are measured and used to reliably identify a particular microorganism assigning a "score value" (Bruker) or a "confidence value" (bioMe´rieux) to each match based on the test organism's similarities to reference spectra [25-27]. In our specific case, these methods are not needed first because the bacteria under study are exactly known (E. coli ATCC 29225) and second because no information on lipid profile could be obtained.

Actually, there is an emerging interest in developing new analytical methods for lipid analysis aimed to identify bacterial taxonomy, to understand the membrane structure, to follow growth changes and metabolic processes, to highlight differences of the same species under normal or stressed growth conditions [~~26, 27~~ 28,29]. In this work, the first goal was to generate reproducible protocols for MALDI TOF MS analysis of both protein and lipid fractions from bacteria aimed at monitoring molecular modifications. At first, the main critical experimental parameters (selection of the MALDI matrix, optimal solvent composition, sample preparation method, lipid/protein extraction protocol) for the MS analyses were optimized on a selected *E. coli* strain with stable growing conditions. It is worth of note that for lipid analysis a drawback of MALDI MS analysis in positive ion mode is represented by ionization suppression effects exerted by major phospholipids as phosphatidylethanolamines (PEs) towards scarcely ionized lipids as phosphatidylglycerols (PGs) and cardiolipins (CLs). To reduce such suppression effects, the analyses were carried out also in negative ion mode by using a binary matrix composed of 1,8-bis(dimethylamino)naphthalene and 9-aminoacridine [~~28,29~~ 30,31]. The resulting procedure was then used to achieve protein/lipid fingerprints from intact *E. coli* after exposure to different Cu salt and nanoparticle loadings. The

results showed differences in spectral pattern of lipids when bacteria were exposed to copper salts and of proteins for bacteria exposed to CuNPs suggesting a different mode of action from the two antimicrobials. Of course, the AM effects were more significant with increasing copper loading and decreasing bacterial concentrations. Finally, as a comparison, the copper bactericidal activity was also evaluated by classical microbiological protocols, such as plate count.

We believe that the presented analytical protocol could allow, in the future, the development of new NAMs with tunable activity in terms of high antimicrobial efficacy and low cytotoxicity, reducing risks for consumer health and improving food safety.

MATERIAL AND METHODS

Materials. 1,8-bis-(dimethyl-amino)naphthalene (DMAN, proton sponge), 2,5-dihydroxybenzoic acid (DHB), α-cyano-4-hydroxycinnamic acid (CHCA), α-cyano-4-chlorocinnamic acid (CClCA), MRFA, Leucine Enkephalin, Bradykinin (1-7), insulin b chain, insulin, cytochrome c, copper chloride, sodium chloride, copper sulfate pentahydrate ($CuSO_45H_2O$, ≥ 98%), D-(+)-glucose (≥ 99.5%), NaOH (≥ 99.0%) were obtained from Sigma-Aldrich (Sigma Aldrich, St. Louis, MO, USA). 9-aminoacridine hemihydrate was purchased from Acros Organics (Morris Plains, NJ). All the reagents (TraceSelect®) were purchased from Sigma Aldrich. Water, acetonitrile (ACN), trifluoroacetic acid (TFAA), methanol (MeOH), and chloroform (Sigma Aldrich) were LC-MS grade and were used without further purification. All aqueous solutions for CuNPs synthesis were prepared in ultrapure water (Millipore, 18.2 MΩ).

Bacteria growth

E. coli (ATCC 29225) standard culture bacteria were obtained from LGC ATCC Standards (LGC Standards S.r.l., Milano, Italy). Glassware and media were subjected to autoclave at 15 lbs of pressure for 15 min prior to bacteria culture. One colony of *E. coli* was carefully taken up from a freshly prepared using a sterile loop. The collected bacteria were cultured on Nutrient Broth (Oxoid) for 48 h at 42 °C up to a cell density of typically 10^{10} cells/mL. Serial dilutions were set up in saline solution (NaCl 0.9%) and 1 mL of the resulting dilution was inoculated into nutrient medium (Nutrient Agar Oxoid); the plates were then incubated at 42° C for 24 h. After the incubation, the colonies were counted for each dilution, and the concentration of *E. coli* was deduced from the primary culture broth. To each dilution, $CuCl_2$ (10 ppm, 1 ppm and 0.5 ppm) or CuNPs (1 ppm and 0.5 ppm) were added and left at 42° C for 4 hours. Control samples were grown in exactly the same conditions.

Synthesis of copper nanoparticles

Copper nanoparticles (CuNPs) were synthesized according to a wet-chemical protocol reported in literature [~~30~~ 32]. Copper sulfate pentahydrate was used as precursor of CuNPs and D-(+)-glucose was employed as reducing agent. NaOH 1 M solution was used to raise pH. Briefly, 10 µL of NaOH 1 M were added to 5 mL glucose solution (0.04 g/mL) heating the mixture at 60°C in a thermostated mineral oil bath, under stirring. Afterwards, 200 µL of copper sulfate solution (0.01 M) were also added raising the temperature to 80°C, and keeping the reaction for 10 minutes. In this step, solution turned yellowish indicating CuNPs formation. A controlled nitrogen atmosphere was kept during the synthesis.

Spectroscopic and morphological characterization of CuNPs

UV-Vis spectra of the as-prepared CuNPs were registered on a double-beam spectrometer (Shimadzu UV-1601) from 300 to 800 nm, with 1-cm Quartz Suprasil® cuvettes (Hellma Analytics). Their morphological characterization was carried out by Transmission electron microscopy (TEM) using a FEI Tecnai 12 instrument (120 kV; filament: LaB6). 5-µL sample was deposited on Formvar®-coated Cu grid (300 mesh, Agar Scientific). Colloid concentration was assessed by means of Electrothermal Atomic Absorption Spectroscopy (ETAAS) with a Perkin Elmer PinAAcle 900Z apparatus equipped with a Cu hollow cathode lamp. Calibration curve in the range 0-50 ppb was registered using a 50 ppb copper standard solution prepared in HNO_3 0.2%w, automatically diluted by Perkin Elmer AS800 autosampler. Cu 1000 ppm solution (Perkin Elmer) was used as stock.

MALDI Matrices Solution – The selected matrices for protein analysis were prepared at a concentration of 50 mM in 70:30 acetonitrile/water with 1.25% TFA, while the selected matrices

for lipid analysis were prepared at the same concentration in methanol. The binary DMAN/9AA matrix (equimolar mixture) was obtained by properly mixing the above stock solutions (50 mM each in methanol). For analyte-matrix mixture, different deposition strategies were tested. Best results were achieved following the premix (volume or one layer) method, in which the bacteria suspension (usually 5 µL) and matrix solution (5 µL) are transferred and mixed in an Eppendorf tube by vortexing for a few seconds before depositing the mixture onto the plate and then allowed to air-dry at room temperature. This method is also reported as dried-droplet by many investigators.

Protein extraction. After testing different methods of protein extraction the following protocol was used: 500 µL of bacterial culture were centrifuged at 15.000 rpm for 5 min to pellet the cells. The supernatant was discarded; the cells were washed twice with 1 mL of water. After each step, the cells were pelleted by centrifugation at 15.000 rpm for 5 min. The pellet was dissolved by vortexing for 2 min in 50-100 µL of 1.25% TFA.

Lipid extraction. For lipids extraction two procedures were adopted after obtaining the cell pellet as described before. In the first, following the Bligh-Dyer method ~~[31~~ 33], the pellet was resuspended in 100 µL of water. 150 µL of $CHCl_3$/MeOH (1:2) were added followed by vigorous vortex-mixing and ultrasonication (20 min). Then, 50 µL of $CHCl_3$ followed by 50 µL of H_2O were added and the mixture was vortexed and ultra-sonicated again (20 min) after each addition. Finally, the mixture was centrifuged (10 min at 3000×g) to facilitate phase separation. The lower organic layer was collected, concentrated under a nitrogen stream, reconstituted into 100 µL of a $CHCl_3$/MeOH (1:1) solution and prepared for lipid MALDI analysis in positive ion mode using DHB or CClCA as a matrix. In the second protocol, the pellet was resuspended in 20 µL of the methanolic solution of DMAN matrix, vortexed and ultra-sonicated (10 min); after 20 µL of 9AA methanolic solution were added and the mixture vortexed and ultra-sonicated again (10 min). 1 µL of the suspension was spotted directly on the target plate and analyzed by MALDI-TOF-MS.

MALDI TOF MS

MS experiments were performed using a Micromass M@LDI™ - LR time-of-flight mass spectrometer (Waters MS Technologies, Manchester, UK) equipped with a nitrogen UV laser (337 nm wavelength), a precision flat target plate sample introduction system bearing a micro-titer target plate, reflectron optics and a fast dual micro-channel plate (MCP) detector.

In positive ion mode (reflectron and linear) the following voltages were applied: pulse, 2610 V (1400 V); source, 15000 V (15000 V); reflectron, 2000 V; MCP 1900 V (1900 V) for reflectron (linear) mode. For negative mode (only in reflectron) a supply voltage of 5000 V was applied. The laser firing rate was 5 Hz, and, unless otherwise specified, 60 laser shots, obtained by a random rastering pattern, were used for each well. The resulting spectra were averaged, background subtracted, and smoothed by a Savitzky Golay algorithm in reflectron mode and a mean algorithm in linear mode. A time lag focusing (TLF) delay of 500 ns was used. Mass calibration in reflectron mode was performed using a peptide mixture composed of MRFA, Leucine Enkephalin acetate salt hydrate, Bradykinin (1-7). External mass calibration in linear mode was performed using a protein mixture composed of insulin b chain, insulin and cytochrome c. Cyt c was also used to internally calibrate protein sample spots.

The optimized method has been applied on different cultured bacteria prepared during one year of work. The spectra have been acquired in triplicate for each culture broth. The analyses have been carried out on 5 dilutions for each culture with a total of 45 analyses for each culture. The spectra were always externally and internally calibrated for each spot as described.

Results and discussion

1. *E. coli* protein analysis

First of all, the protocol was adjusted for the extraction and the analysis of proteins, which represent the characteristic and easily accessible biomarkers from microorganisms, with the aim to obtain as many signals as possible. The critical factors influencing the measurements of mass spectrometric peptide/protein profiles from *E. coli* were evaluated, such as cell concentration, selection of suitable matrix compounds, matrix solvent systems, additives influencing the release of marker peptides and proteins from the cell wall, and MALDI sample preparation methods. The first attempts consisted in evaluating the proper cell concentration starting from 10^{10} cell/mL down to 10^{3} cells/mL applying conventional conditions (extraction in TFA 0.1%, matrix CHCA in ACN 70:30, TFA 0.1%). Reproducible results were obtained by using concentration of bacteria from 10^{9} to 10^{6} cells/mL, while lower concentration resulted in a different protein profiling in terms of number of peaks and peak relative intensity. Then, several MALDI matrices (DHB, CHCA and CClCA) were tested on a selected cell concentration (10^{8} cells/mL). By using DHB, high intensity signals in the low *m/z* range (<5000) were observed employing higher laser fluence compared to CHCA and CClCA with evident phenomena of hot spot due to inhomogeneous crystallization. Among CHCA and CClCA the latter was selected as the best matrix since it allowed to detect a higher number of peptides/proteins in the whole investigated range thanks to its ability in ionizing less basic peptides compared to the classical CHCA [~~32~~ 34]. Another critical factor in biotyping analyses is represented by the use of strong organic acid for cell lysis and the consequent release of proteins from the cell membrane [~~33~~ 35]. We have studied, therefore, the effect of a variable concentration of TFA both in the mixture of solvents used to dissolve CClCA matrix and in the cell pellet resuspension solution. Initially, TFA concentration was kept constant in the cell resuspension solution (0.1%) and varied at 2.5 %, 1.25 % and 0.1 % in the solvent mixture of MALDI matrix.

The MALDI spectra obtained under these conditions are shown in Figure 1A-C, respectively. It can be noted that 0.1% TFA allows the preferential ionization of lower m/z peptides (Fig 1C), while 2.5% TFA caused a detrimental effect on signal-to-noise ratio on the whole mass range (Fig. 1A). This outcome may be related to the ion-pairing nature of TFA that at high concentration could strong interact with the matrix molecules reducing the global ionization yield. Enhanced spectra in terms of signal intensity and number of detected ions, mainly in the *m/z* range 8000-15000, were experienced by using an intermediate 1.25% TFA concentration (Fig. 1B) that was then used through this work. Thus, the concentration of TFA was kept constant in the matrix (1.25%) and varied at 2.5%, 1.25% and 0.1% in the resuspension pellet. The MALDI spectra obtained in these conditions are reported in Figure 1D-F, respectively. It is clear as the lowest TFA concentration (0.1%) already disrupts partly the cell wall and causes a certain release of cell proteins (Fig 1F). In particular, note the reproducibility in Fig 1B and Fig 1F which are referred to the same conditions of TFA 0.1% (pellet) -TFA1.25% (matrix) also if prepared on different cell collections. Contrary, the higher TFA concentration (2.5%) caused cell spoilage with degradation of proteins at high *m/z* values and appearance of more peptide signals at lower *m/z* range (Fig 1D). The mass spectrum relevant to 1.25% TFA (Fig. 1E) shows a protein profile more informative with higher signal intensity and number of peaks in the region 8000-17000 *m/z*. So the variation of TFA concentration significantly modifies the protein profile; the best results were achieved with both concentrations of TFA at 1.25%. The final investigated step in the sample preparation protocol was the sample deposition onto the MALDI plate, and three methods were tested: dried droplet, pre-mixed volume, and over-layer or two-layer. The pre-mixed volume and dried droplet methods provided comparable results in agreement with previous reports [~~33, 34~~ 35, 36] with a more homogenous surface than two layers, which was also time consuming and less reproducible. However, the pre-mixed method was selected for further analyses to ensure a more intimate contact between cells and matrix solution. At the end, we observed a significant number of protein ions in the present study. The

probable attribution of these signals was supported by querying the ExPASy database through the TagIdent tool (http://web.expasy.org/tagident/) and by literature [37-40].

2. *E. coli* lipid analysis

The experimental conditions optimized for protein profiling were applied then for lipid analysis. Note that also for lipids the use of CClCA as a matrix was preferred since less laser fluence was necessary and less signal spreading in sodiated and potassiated forms was experienced compared to DHB (data not shown). A typical mass spectrum of the Bligh Dyer lipid extract from *E. coli* ATCC25922 analyzed in positive ion mode with CClCA as a matrix is shown in Figure 2A. Previous reports on *E. coli* LM 3118 [~~35~~ 41], K12 [~~36~~ 42], and TOP10 [~~37~~ 43] strains assessed that the major phospholipids (PLs) present in cell membrane are phosphatidylethanolamines (PEs) and phosphatidylglycerols (PGs). Here, the *m/z* range between 620 and 800 includes ions that are consistent with these assignments. For instance, the signal at *m/z* 690.50 could correspond to the protonated ion of PE (C15:0/cyC17:0) or (C16:0/C16:1) [~~35~~ 41], the signal at *m/z* 704.50 could be attributed as protonated PE (C16:0/cyC17:0) [~~35~~ 41], with its sodiated adduct at *m/z* 726.51. The *m/z* range between 500 and 610 includes ions that are consistent with the PEs and PGs following the loss of polar headgroup. For example, the signals at *m/z* 549.49 and 563.51 are derived from *m/z* 690.50 and 704.50 respectively, after the loss of the ethanolamine phosphate head-group [$(C_2H_5N)H_3PO_4$] (141 amu). To be confident of the previous attributions, information about fatty acids in the lower *m/z* range would be needed. However, the investigation of the 200-350 *m/z* range is typically hindered in positive ion mode due to the dominant interfering signals from the used organic matrix. To this aim, the lipid extract was processed and analyzed in negative ion mode by using the binary matrix (see above). This matrix produces a few interfering ions and promotes only deprotonated ions avoiding the formation of sodiated and potassiated adducts which decrease the sensitivity and complicate the interpretation of the spectrum. Fig 2B reports the relevant MALDI

spectrum in the *m/z* range 400-800 as a comparison with positive ion mode. It was possible to detect again the previous observed PEs as deprotonated molecules. Moreover, a higher number of ions attributed as PGs were observed thanks to a reduced suppression effects from PEs in negative ion mode (see Table 1). The *m/z* range from 200 to 350 includes (see Figure 2C) signals consistent with the assignment as carboxylate anions formed from phospholipids or present as free fatty acids (FFAs). Previous studies reported that *E. coli* typically contains the following constituent FFAs: C10:0, C12:0, C14:0, C16:0, C16:1, C18:0, C18:1 and C18:1, and, to a lesser extent, of C15:0, C17:0, cyclopropane (*cyc*-$C_{17:0}$) and (*cyc*-$C_{19:0}$) [~~38~~ 44]. In our case, we observed signals at *m/z* 227, 253, 255, 267, 281, 283, 295, attributable to C14:0, C16:1, C16:0, cyc-C17:0, C18:1, C18:0, cyc-C19 carboxylate anions together with intense signal ions at *m/z* 311, 325, 339 that could correspond to higher FFA carboxylate anions. Additionally, with this matrix we were able also to detect cardiolipins in the *m/z* range 1340–1500 (Fig 2D), minor constituents of *E. coli* membrane [~~39~~ 45]. A complete list of the lipids observed in Figure 2A-D with their most probable attributions is reported in Table 1. Lipid assignments were aided by using the LIPID MAPS (http://www.lipidmaps.org/) and METLIN (http://metlin.scripps.edu/) databases and literature [~~35-39~~ 41-45].

3. Protein analysis after NAM exposure

In our first experiments, different copper salt concentrations (0.5 ppm, 1 ppm, 10 ppm) were applied to a cell concentrations range of *E. coli* and left in contact for 4 hours before sample processing and MALDI analysis. This contact time was chosen since our previous studies on copper antimicrobial effect [7] revealed the plateau achievement in copper killing effect after 4 hrs. Figure 3 reports the MALDI mass spectra of control samples (A) and bacteria after exposure to 10 ppm of $CuCl_2$ (B) (initial bacteria concentration 10^9 cell/mL). The majority of detected peaks corresponded to highly abundant ribosomal proteins according to previous reports [~~40~~ 37 and references herein].

The analyses of the spectra revealed a negligible effect of copper on high concentrated bacteria in terms of observed ions and relative peak abundances (for copper at 0.5 and 1 ppm *vs* control no difference was found). However, the punctual inspection of the spectra allowed discovering a few differences in some proteins (see insets a-d in Fig. 3) that were observed in all the three replicates. In particular, it was possible to detect, only in treated samples, a signal at *m/z* 4920 *(inset a)* that is most likely the bi-charged ion of the signal at *m/z* 9840 *(inset d)*, a peak at *m/z* 6178 *(inset b)*, and a little shoulder at *m/*z 7348 *(inset c)*. ~~We tried to attribute these signals querying the ExPASy database through the TagIdent tool (http://web.expasy.org/tagident/).~~ By recurring to TagIdent tool and by selecting the organism species *E. coli*, the ion at *m/z* 6178 (~~mass tolerance 0.01%~~ Mw range (in percent): 0.01 %) was attributed as uncharacterized protein or putative transposase which is a DNA binding protein that could be overexpressed as cellular response to DNA damage stimulus. The ion at *m/z* 7348 could be interpreted both as the oxidation of the peak at *m/z* 7332 which is a cold shock-like protein CspE [~~40~~ 37] or as a new protein attributed as uncharacterized protein or antitoxin of toxin-antitoxin stability system which is linked to genes whose expression inhibits cell growth and causes cell death when overproduced [~~41~~ 46]. Very interestingly, for the *m/z* 9840 value, the following proteins were proposed as first candidates: cation efflux system protein CusF and copper-binding protein. The first protein is located in the outer membrane-bounded periplasmic space and is reported to mediate resistance to copper and silver by cation efflux. A specific study [~~42~~ 47] reported that CusF could be detected in periplasmic extracts of *E. coli* strains only after induction with $CuCl_2$ and the size of the detected protein was about 10 kDa, in fully accordance with our findings. Also the copper-binding protein is periplasmic and could be overexpressed for protecting *E. coli* cells from copper-induced cellular damage [~~43~~ 48]. An indirect support to the occurrence of *cusF* is given by Yamamoto et al., in a previous study on transcriptional response of *E. coli* upon exposure to external copper using DNA microarray and transcription assays [49]. It was found out that the copper stimulus involved at least 21 induced genes in cellular processes for

detoxification of copper, including seven genes for transporters as *cusB, cusC, cusF, copA, ebr, yccA* and *yeeF*. It is possible to correlate this stimulation to our study since the gene cusB is coding for the cation efflux system protein *cusF*.

Afterwards, stress response on *E. coli* was evaluated by testing aqueous copper nanocolloids. An easy approach for the preparation of CuNPs was selected with a particular focus on the stabilizing agent involved in the synthesis. Glucose can play the dual role of capping and reducing agent in the presence of a Cu (II) salt as precursor of NPs [~~30~~ 32]. Moreover, it does not influence the bacterial culture medium. The as-synthesized NPs were characterized by UV-Vis and TEM. Typical UV-Vis spectrum (a) and TEM micrograph (b) of CuNPs are reported in Fig. 4. The observed absorption band is well below the value reported for copper plasmon peak (~570 nm), but is compatible with very small copper nanoclusters (≤ 4 nm) which generally show featureless absorption at lower wavelengths [~~44, 45~~ 50,51]. In fact, the reduced size of CuNPs was assessed by TEM analysis finding NP diameters in the range between 1 and 4 nm. As said, *E. coli* was exposed to 0.5 ppm and 1 ppm of the freshly prepared CuNPs. Additionally, the experimental concentration of CuNPs was evaluated by means of ETAAS characterization giving 32.6±0.8 ppm. CuNP concentration was determined in the supernatant obtained after pelleting bacterial culture giving the experimental value of added copper colloid (0.65±0.15 and 1.3±0.3 ppm) in place of the theoretical additions of 0.5 and 1 ppm, respectively.

Remarkably, from the MALDI spectra registered for control (Fig 5A) and for bacteria exposed to 1 ppm of CuNPs (Fig 5B) (initial bacteria concentration 10^9 cell/mL) it was possible to observe the same protein modifications induced by copper salts. Therefore, when *E. coli* at high concentration were exposed to NAMs, most of ribosomal proteins are conserved but a first adaptation mechanism is perceived by the overexpression of proteins related to copper stress response. Moreover, as expected, when using CuNPs the same effect was exerted at lower concentration compared to

copper salt, due to their small size and high surface-to-volume ratio, which allow them to interact closely with *E. coli* membranes. It is worth of note that when analysing high concentrated bacteria after contact with 0.5 ppm CuNPs a global enhancement of MALDI-MS signals intensity was observed (data not shown) suggesting also for copper a bifunctional property in acting as affinity probes at lower concentrations and bactericidal at higher concentrations, as previously demonstrated for AgNPs [~~46~~ 52] and ZnONPS [~~47~~ 53]. Probably this copper concentration is sufficient to unfold the proteins at denaturation state and enhance their ionization efficiency without inducing significant modifications. The same analyses were repeated for less concentrated bacteria (10^7 cell/mL) that should perceive a more marked antibacterial effect from salt and CuNPs. The mass spectra of untreated sample (A) and treated with 10 ppm of $CuCl_2$ (B) and untreated sample (C) and treated with 1 ppm CuNPs (D) are reported in Fig. 6. In this case, apart from the proteins discussed before, it was possible to notice a general degradation of S/N ratio and the disappearance of signals at higher *m/z* range due to a degradation of ribosomal membrane proteins. This effect is more pronounced in bacteria treated with CuNPs as already explained. It is also interestingly to notice that the signal at *m/z* 9840 (cation efflux system protein CusF) continues to increase in stressed bacteria (Figure 7 A-D). These preliminary findings indicate as several proteins appear over- or under-expressed in the different treatments; future work will be addressed in collecting more data to perform a post-processing statistical analysis for discriminating protein markers of stress.

4. Lipid analysis after NAM exposure

Bacteria exposed to the copper salt show peculiar lipid profiles, characterized by a complete degradation of lipids observed in control samples (see Fig. 2) and the simultaneous appearance of oxidation by-products (Fig. 8A,C). These ions appearing in the *m/z* window ranging from 600 to 860 are probably due to secondary oxidation products originating from β-scission reactions involving epoxides, hydroperoxides or peroxides. Indeed, the hydroxyl radicals (OH) generated in

presence of copper are capable to drive the nonenzymatic peroxidation of the unsaturated double bonds of fatty acids, thereby initiating a series of reactions that result in extensive structural changes of the phospholipid bilayer and loss of membrane integrity [22]. This effect is more marked when analyzing the lipids in positive ion mode, probably because the lipids were partially degraded already in the control samples (see Fig. 2A) due to the acidic matrix used. For instance, it is reported for cholesterol analysis that, when using acidic matrices such as DHB, CClCA and CHCA, artifacts can be originated due to analyte oxidation initiated by hydroxyl radicals generated upon laser irradiation of the matrix itself [~~48~~ 54]. So, in this case, an enhanced degradation could be due to both the use of acidic matrix and the presence of copper salt. Indeed, in negative ion mode, where basic matrices are used, this strong oxidation is not observed; it is possible to still detect some PGs and PEs with very low intensity suggesting their degradation (Fig. 8B, D) while less abundant cardiolipins are no more detectable. A common feature between positive and negative spectra is represented by the occurrence of very intense ions at *m/z* 1293.59 (positive) and *m/z* 1291.59 (negative). This peak could be probably ascribed to the class of membrane extrapolysaccharides [~~49~~ 55] which usually protect bacteria from predators and environmental stresses (certain attribution needs of course further investigations by tandem MS analysis). Contrary to these findings, investigations carried out on lipids extracted from *E. coli* exposed to CuNPs showed spectral pattern almost unaffected similar to the one observed in Figure 2, with a marginally decrease in signal intensity suggesting a limited degradation action. Thus, from these investigations it seems that oxidation of membrane phospholipids is the primary mediator of copper killing effect when soluble salts are used as antimicrobial.

Finally, the antimicrobial action was monitored also by conventional microbiological tests (plate counting). The number of CFUs (colony forming units) within the resulting suspensions was enumerated after 4 h of incubation. Results demonstrate a slight activity of both $CuCl_2$ and CuNPs

compared to the control strains when *E. coli* with initial concentration of 10^7 cell/mL was analyzed. Indeed, in this case, the *E. coli* colonies showed a cell load from 1000 to 100 CFU/mL after incubation with copper. This means that copper can exert its antimicrobial activity even if part of bacteria can repair membrane damage or are not damaged completely. Indeed, at this concentration, we could detect degradation of higher proteins in MALDI spectra but it was still possible to observe many stable proteins. When the ratio between cells number and copper concentration diminished, of course the antimicrobial effect was stronger. Indeed, when analyzing bacteria with lower initial concentration (10^6 cell/mL) after copper exposure no signal related to intact proteins was detected. These experimental findings from mass spectra analyses were confirmed also by microbiological assay since the CFU/mL in those cases was found to be zero indicating a complete killing effect from copper.

Conclusions

MALDI TOF mass spectrometry revealed as a powerful tool for the identification of protein and lipid cell membrane damage in *E. coli* exposed to different copper-based antimicrobial agents. Bacteria exposed to different copper loadings showed interesting results demonstrating over-expression of copper binding proteins. Moreover, a complete degradation of lipids was achieved when treating the bacteria with soluble salt, indicating that in this case the oxidation of membrane phospholipids is the primary mediator of copper killing effect. MALDI-MS can overcome the limitations faced by the conventional techniques and offers a powerful tool to rationalize microbial response to stress conditions.

Acknowledgment

Ms. Tania Pellegrini is gratefully acknowledged for partial support in running experiments.

References

[1]. K.J. Kennedy, J.L. Roberts, P.J. Collignon. Escherichia coli bacteraemia in Canberra: incidence and clinical features. *Med. J. Aust.* **2008**, *188*, 209.

[2]. R.L. Vogt, L. Dippold. Escherichia coli O157:H7 outbreak associated with consumption of ground beef, June-July 2002". *Public Health Rep.* **2005**, *120*, 174.

[3]. H.M. Al-Qadiri, M. Lin, A.G. Cavinato, B.A. Rasco. Fourier transform infrared spectroscopy, detection and identification of Escherichia coli O157: H7 and Alicyclobacillus strains in apple juice. *Int. J. Food Microbiol*. **2006**, *111*, 73.

[4]. J. Lin, M. P. Smith, K. C. Chapin, H. S. Baik, G. N. Bennett, J. W. Foster, Mechanisms of acid resistance in enterohemorrhagic Escherichia coli. *Appl. Environ. Microbiol*. **1996**, *62*, 3094.

[5] P. Collignon. Resistant Escherichia coli-We Are What We Eat. *Clin Infect Dis*. **2009**, *49*, 202.

[6] N. Beyth, Y. Houri-Haddad, A. Domb, W. Khan, R. Hazan. Alternative Antimicrobial Approach: Nano-Antimicrobial Materials. *Evid.-based Compl. Alt.* **2015**, *2015*, 1.

[7] N. Cioffi, N. Ditaranto, L. Sabbatini, L. Torsi, P.G. Zambonin. Nanomaterials for metal controlled release and process for their production. E.P. app. n. 08425299.8, date of filing 29.04.2008

[8] M.C. Sportelli, R.A. Picca, N. Cioffi. *Nano-Antimicrobials Based on Metals, in Novel Antimicrobial Agents and Strategies* Wiley-VCH Verlag GmbH & Co. **2014**

[9] D. Longano, N. Ditaranto, N. Cioffi, F. Di Niso, T. Sibillano, A. Ancona, A. Conte, M.A. Del Nobile, L. Sabbatini, L Torsi. Analytical characterization of laser-generated copper nanoparticles for antibacterial composite food packaging. *Anal. Bioanal. Chem.* **2012**, *403*, 1179.

[10] G. Grass, C. Rensing, M. Solioz. Metallic copper as an antimicrobial surface. *App. Environ. Microb.* **2011**, *77*, 1541.

[11] J.O. Noyce, H. Michels, C.W. Keevil. Inactivation of influenza A virus on copper versus stainless steel surfaces. *Appl. Environ. Microbiol*. **2007,** *73*, 2748.

[12] L. Weaver, H.T. Michels, C.W. Keevil. Potential for preventing spread of fungi in air conditioning systems constructed using copper instead of aluminium. *Lett. Appl. Microbiol.* **2009**, *50*, 18.

[13] M.M.O. Pena, K.A. Koch, D.J. Thiele. Dynamic regulation of copper uptake and detoxification genes in Saccharomyces cerevisiae. *Mol. Cell. Biol.* **1998,** *18*, 2514.

[14] J.J. Harrison, V. Tremaroli, M.A. Stan, C.S. Chan, C. Vacchi-Suzzi, B.J. Heyne, M.R. Parsek, H. Ceri, R. J. Turner. Chromosomal antioxidant genes have metal ion-specific roles as determinants of bacterial metal tolerance. *Environ. Microbiol*. **2009,** *11*, 2491.

[15] J.A. Imlay. Pathways of oxidative damage. *Annu. Rev. Microbiol*. **2003**, *57*, 395.

[16] Z. Vardanyan, A. Trchounian. The effects of copper (II) ions on Enterococcus hirae cell growth and the proton-translocating FoF1 ATPase activity. *Cell Biochem. Biophys*. **2010**, *57*, 19.

[17]. M. Nyden, C. Fant. PCT Int. Appl. Application: WO 2006-SE318 20060313. **2006,** 27 pp.

[18]. J. Lin, C.Y. Yang, C.C. Chou, H.L. Su, T.J. Hung. U.S. Pat. Appl. Publ. Application: 994 US 2008–253037 20081016. **2009**, 27 pp.

[19]. L. Macomber, C. Rensing, J. A. Imlay. Intracellular copper does not catalyse the formation of oxidative DNA damage in E. coli. *J. Bacteriol*. **2006**, *189*, 1616.

[20]. J.P. Ruparelia, A.K. Chatterjee, S.P. Duttagupta, S. Mukherji. Strain specificity in antimicrobial activity of silver and copper nanoparticles. *Acta Biomat,* **2008**, *4*, 707.

[21]. L. Esteban-Tejeda, F. Malpartida, A. Esteban-Cubillo, C. Pecharroman, J.S. Moya. Antibacterial and antifungal activity of a soda-lime glass containing copper nanoparticles. *Nanotech.* **2009**, *20*, 505701.

[22]. R. Hong, T.Y. Kang, C.A. Michels, N. Gadura. Membrane Lipid Peroxidation in Copper Alloy-Mediated Contact Killing of Escherichia coli. *Appl. Environ. Microbiol*. **2012**, *78*, 1776.

[23]. N. AlMasoud, Y. Xu, N. Nicolaou, R. Goodacre. Optimization of matrix assisted desorption/ionization time of flight mass spectrometry (MALDI-TOF-MS) for the characterization of Bacillus and Brevibacillus species. *Anal. Chim. Acta* **2014**, *840*, 49.

[24]. M.T. Gekenidis, P. Studer, S. Wuthrich, R. Brunisholz, D. Drissner. Beyond the MALDI biotyping workflow: in search of microorganism-specific tryptic peptides enabling discrimination of subspecies. *Appl. Environ. Microbiol.* **2014**, *80*, 4234.

[25] T.C. Dingle, S.M Butler-Wu. MALDI-TOF mass spectrometry for microorganism identification. *Clin. Lab. Med.* **2013**, *33*, 589.

[26] C. A. Mather, S. F. Rivera, S. M. Butler-Wu. Comparison of the Bruker Biotyper and Vitek MS Matrix-Assisted Laser Desorption Ionization–Time of Flight Mass Spectrometry Systems for Identification of Mycobacteria Using Simplified Protein Extraction Protocols. *J. Clin. Microbiol.* **2014,** 52, 130.

[27] M.L. De Marco, B.A. Ford. Beyond identification: Emerging and future uses for maldi-tof mass spectrometry in the clinical microbiology laboratory. *Clin. Lab. Med.* **2013**, *33*, 611.

[28] C. D. Calvano, F. Italiano, L. Catucci, A. Agostiano, T. R. I. Cataldi, F. Palmisano, M. Trotta, The lipidome of the photosynthetic bacterium Rhodobacter sphaeroidesR26 is affected by cobalt and chromate ions stress *Biometals* **2014**, *27*, 65.

[29] S. K. Kailasa, H-F. Wu. Surface modified $BaTiO_3$ nanoparticles as the matrix for phospholipids and as extracting probes for LLME of hydrophobic proteins in Escherichia coli by MALDI–MS *Talanta* **2013**, *114*, 283.

[30] C.D. Calvano, C.G. Zambonin, F. Palmisano. Lipid fingerprinting of Gram-positive lactobacilli by intact cells–matrix-assisted laser desorption/ionization mass spectrometry using a proton sponge based matrix. *Rapid Comm. Mass Spectrom*. **2011**, *25*, 1757.

[31] C.D. Calvano, A. Monopoli, N. Ditaranto, F. Palmisano. 1,8-Bis (dimethylamino) naphthalene/9-aminoacridine: a new binary matrix for lipid fingerprinting of intact bacteria by matrix assisted laser desorption ionization mass spectrometry. *Anal. Chim. Acta* **2013**, 798, 56.

[32] S. Panigrahi, S. Kundu, S. K. Ghosh, S. Nath, S. Praharaj, S. Basu, T. Pal. Selective one-pot synthesis of copper nanorods under surfactantless condition. *Polyhedron* **2006**, *25*, 1263.

[33] E.G. Bligh, W.J. Dyer. A rapid method of total lipid extraction and purification. *Can. J. Biochem. Physiol.* **1959,** 37, 911.

[34] T.W. Jaskolla, W.D. Lehmann, M. Karas. 4-Chloro-α-cyanocinnamic acid is an advanced, rationally designed MALDI matrix. *Proc. Natl. Acad. Sci. U.S.A*. **2008**, *105*, 12200.

[35] J. Chalupová, M. Sedlárová, M. Helmel, P. Rehulka, M. Marchetti-Deschmann, G. Allmaier, M. Šebela. MALDI-based intact spore mass spectrometry of downy and powdery mildews. *J. Mass. Spectrom.* **2012**, *47*, 978.

[36] J. Kemptner, M. Marchetti-Deschmann, C.P. Kubicek, G. Allmaier. Mixed volume sample preparation method for intact cell mass spectrometry of Fusarium spores. *J. Mass Spectrom*. **2009**, *44*, 1622.

[37] R.A. Momo, J.F. Povey, C. M. Smales, C. J. O'Malley, G.A. Montague, E.B. Martin. MALDI-ToF mass spectrometry coupled with multivariate pattern recognition analysis for the rapid biomarker profiling of Escherichia coli in different growth phases. *Anal. Bioanal. Chem*. **2013**, 405, 8251.

[38] Z. Wang, K. Dunlop, S. R. Long, L. Li. Mass Spectrometric Methods for Generation of Protein Mass Database Used for Bacterial Identification. *Anal. Chem.* **2002***, 74,* 3174.

[39] M. Sauget, M.-H. Nicolas-Chanoinec, N. Cabrolier, X. Bertrand, D. Hocquet. Matrix-assisted laser desorption ionization-time of flight mass spectrometry assigns Escherichia coli to the phylogroups A, B1, B2 and D. *Int. J. Med. Microbiol.* **2014**, *304*, 977.

[40] C. G. Clark, P. Kruczkiewicz, C. Guan, S. J. McCorrister, P. Chong, J. Wylie, P. van Caeseele, H. A. Tabor, P. Snarr, M. W. Gilmour,E. N. Taboada, G.R. Westmacott. Evaluation of MALDI-TOF mass spectroscopy methods for determination of *Escherichia coli* pathotypes. *J. Microbiol. Meth*. **2013**, *94*, 180.

[41] D. Oursel, C. Loutelier-Bourhis, N. Orange, S. Chevalier, V. Norris, C.M. Lange. Lipid composition of membranes of Escherichia coli by liquid chromatography/tandem mass spectrometry using negative electrospray ionization. *Rapid Commun. Mass Spectrom*. **2007**, *21*, 1721.

[42] J.I. Zhang, N. Talaty, A.B. Costa, Y. Xia, W.A. Tao, R. Bell, J.H. Callahan, R.G. Cooks. Rapid direct lipid profiling of bacteria using desorption electrospray ionization mass spectrometry *Int. J. Mass Spectrom*. **2011**, *301*, 37.

[43] J. Gidden, J. Denson, R. Liyanage, D.M. Ivey, J.O. Lay Jr. Lipid compositions in Escherichia coli and Bacillus subtilis during growth as determined by MALDI-TOF and TOF/TOF mass spectrometry. *Int. J. Mass Spectrom*. **2009**, *283,* 178.

[44] D. Oursel, C. Loutelier-Bourhis, N. Orange, S. Chevalier, V. Norris, C.M. Lange. Identification and relative quantification of fatty acids in Escherichia coli membranes by gas chromatography/mass spectrometry. *Rapid Commun. Mass Spectrom*. **2007**, *21*, 3229.

[45]. T.A. Garrett, A.C. O'Neill, M.L. Hopson. Quantification of cardiolipin molecular species in Escherichia coli lipid extracts using liquid chromatography/electrospray ionization mass spectrometry. *Rapid Commun. Mass Spectrom*. **2012**, *26*, 2267.

~~[46] R.A. Momo, J.F. Povey, C. M. Smales, C. J. O'Malley, G.A. Montague, E.B. Martin. MALDI-ToF mass spectrometry coupled with multivariate pattern recognition analysis for the rapid biomarker profiling of Escherichia coli in different growth phases. *Anal. Bioanal. Chem*. **2013**, 405, 8251.~~

[46] Y. Yamaguchi, J.H. Park, M. Inouye. Toxin-antitoxin systems in bacteria and archaea. *Annu Rev Genet.* **2011**, *45*, 61.

[47] S. Franke, G.Grass, C. Rensing, D.H. Nies. Molecular Analysis of the Copper-Transporting Efflux System CusCFBA of Escherichia coli. *J Bacteriol.* **2003**, *185*, 3804.

[48] N. Shiraishi, M. Nishikimi. Suppression of copper-induced cellular damage by copper sequestration with S100b protein. *Arch Biochem Biophys*. **1998**, *357*, 225.

[49] K. Yamamoto, A. Ishihama. Transcriptional response of Escherichia coli to external copper. *Mol. Microbiol*. **2005**, *56*, 215.

[50] J. Xiong, Y. Wang, Q. Xue, X. Wu. Synthesis of highly stable dispersions of nanosized copper particles using L-ascorbic acid. *Green Chem.* **2011**, *13*, 900.

[51] S. Kapoor, D. K. Palit, T. Mukherjee. Preparation, characterization and surface modification of Cu metal nanoparticles. *Chem. Phys. Lett.* **2002**, *355*, 383.

[52] J. Gopal, H-Fen Wu, C-Hsun Lee. The bifunctional role of Ag nanoparticles on bacteria—a MALDI-MS perspective. *Analyst* **2011**, *136*, 5077.

[53] J. Gopal, H-F. Wu, Y-H. Lee. Matrix-Assisted Laser Desorption Ionization-Time-of-Flight Mass Spectrometry As a Rapid and Reliable Technique for Directly Evaluating Bactericidal Activity: Probing the Critical Concentration of ZnO Nanoparticles As Affinity Probes. *Anal. Chem.* **2010**, *82*, 9617.

[54]. K.M. McAvey, B. Guan, C.A. Fortier, M.A. Tarr, R.B. Cole. Laser-induced oxidation of cholesterol observed during MALDI-TOF mass spectrometry. *J. Am. Soc. Mass Spectrom.* **2011**, *22*, 659.

[55] G. Gedda, J. Gopal, H-Fen Wu. Electrospray ionization and matrix-assisted laser desorption/ ionization mass spectrometric analysis of extrapolysaccharides of Escherichia coli. *Rapid Commun. Mass Spectrom.* **2012**, *26*, 1609.

Captions to figures

Figure 1. MALDI mass spectra of the *E. coli* protein extract: (A) resuspension solution (RS) 0.1% TFA, CClCA in 70:30 ACN/TFA 2.5%, (B) RS 0.1% TFA, CClCA in 70:30 ACN/TFA 1.25%, (C) RS 0.1% TFA, CClCA in 70:30 ACN/TFA 0.1%, (D) RS 2.5% TFA, CClCA in 70:30 ACN/TFA 0.1%, (E) RS 1.25% TFA, CClCA in 70:30 ACN/TFA 0.1% and (F) RS 0.1% TFA, CClCA in 70:30 ACN/TFA 0.1%.

Figure 2. MALDI mass spectra of *E. coli* lipid extract. (A) Positive ion mode, CClCA used as matrix, (B) Negative ion mode, using a binary matrix, (C) Zoom on fatty acids *m/z* range (D) Zoom on cardiolipins *m/z* range. C, D negative ion mode, using a binary matrix.

Figure 3. MALDI mass spectra of *E. coli* protein extract relevant to (A) control sample and (B) bacteria exposed to 10 ppm $CuCl_2$. Insets *a-d:* zooms on specific proteins. Cell concentration 10^9 cell/mL.

Figure 4. Typical UV-Vis spectrum (a) and TEM micrograph (b) of in house synthesized CuNPs.

Figure 5. MALDI mass spectra of *E. coli* protein extract relevant to (A) control sample and (B) bacteria exposed to 1 ppm CuNPs. Insets *a-d:* zooms on specific proteins. Cell concentration 10^9 cell/mL.

Figure 6. MALDI mass spectra of *E. coli* protein extract relevant to (A) control sample, (B) bacteria exposed to 10 ppm $CuCl_2$, (C) control sample and (D) bacteria exposed to 1 ppm CuNPs. Cell concentration 10^7 cell/mL.

Figure 7. Zoom on *m/z* 9840 for (A) control sample, (B) bacteria exposed to 10 ppm $CuCl_2$, (C) control sample and (D) bacteria exposed to 1 ppm CuNPs. Cell concentration 10^7 cell/mL.

Figure 8. MALDI mass spectra of *E. coli* lipid extract relevant to bacteria exposed to 1 ppm $CuCl_2$ in positive (A) and negative mode (B) and to 10 ppm $CuCl_2$ in positive (C) and negative mode (D). Cell concentration 10^7 cell/mL.

Table 1. Probable attribution of the main ions observed in Figures 2A-D.

Theorethical m/z	Observed m/z	Probable attribution	Positive mode	Negative mode
227.202	227.15	$[C(14:0)-H]^-$		x
253.217	253.15	$[C(16:1)-H]^-$		x
255.233	255.15	$[C(16:0)-H]^-$		x
267.268	267.20	$[Cyc-C17-H]^-$		x
281.249	281.20	$[C(18:1)-H]^-$		x
283.264	283.20	$[C(18:0)-H]^-$		x
295.263	295.23	$[Cyc-C19-H]^-$		x
307.264	307.24	$[C(20:2)-H]^-$		x
311.295	311.22	$[C(20:0)-H]^-$		x
325.310	325.25	$[C(21:0)-H]^-$		x
339.326	339.30	$[C(22:0)-H]^-$		x
523.4727	523.44	Loss of headgroup from PE(30:0)	x	
537.4883	537.45	Loss of headgroup from PE(31:0)	x	
549.4883	549.49	Loss of headgroup from PE(32:1)	x	
551.5039	551.49	Loss of headgroup from PE(32:0)	x	
563.5039	563.51	Loss of headgroup from PE(33:1)	x	
575.5039	575.51	Loss of headgroup from PE(34:2)	x	
577.5196	577.51	Loss of headgroup from PE(34:1)	x	
589.5196	589.50	Loss of headgroup from PE(35:2)	x	
591.5352	591.50	Loss of headgroup from PE(35:1)	x	
603.5352	603.51	Loss of headgroup from PE(36:2)	x	
662.4766	662.45	$[PE(30:0)-H]^-$		x
664.4912	664.48	$[PE(30:0)+H]^+$	x	
674.4839	674.48	$[PE(31:1)-H]^-$		x
676.4912	676.50	$[PE(31:1)+H]^+$	x	x
676.4996	676.48	$[PE(31:0)-H]^-$		x
677.4472	677.45	$[PG(29:1)-H]^-$		x
678.5068	678.51	$[PE(31:0)+H]^+$	x	
679.4545	679.47	$[PG(29:1)+H]^+$	x	
686.4737	686.47	$[PE(30:0)+Na]^+$	x	
688.4996	688.51	$[PE(32:1)-H]^-$		x
689.4472	689.51	$[PG(30:2)-H]^-$		x
690.5068	690.50	$[PE(32:1)+H]^+$	x	
690.5079	690.50	$[PE(32:0)-H]^-$		x
692.5225	692.50	$[PE(32:0)+H]^+$	x	
695.4730	695.58	$[PA(36:4)-H]^-$		x
700.4893	700.49	$[PE(31:0)+Na]^+$	x	
702.5152	702.54	$[PE(33:1)-H]^-$		x
704.5225	704.55	$[PE(33:1)+H]^+$	x	
712.4893	712.49	$[PE(32:1)+Na]^+$	x	
714.5152	714.56	$[PE(34:2)-H]^-$		x
716.5225	716.51	$[PE(34:2)+H]^+$	x	
716.5309	716.53	$[PE(34:1)-H]^-$		x
717.5513	717.56	$[PA(37:0)-H]^-$		x
718.5381	718.51	$[PE(34:1)+H]^+$	x	
719.4941	719.52	$[PG(32:1)-H]^-$		x
726.5050	726.51	$[PE(33:1)+Na]^+$	x	
728.5236	728.52	$[PE(35:2)-H]^-$		x

730.5381	730.51	$[PE(35:2)+H]^+$	x	
730.5392	730.58	$[PE(35:1)-H]^-$		x
732.5538	732.51	$[PE(35:1)+H]^+$	x	
733.5025	733.51	$[PG(33:1)-H]^-$		x
740.5206	740.52	$[PE(34:1)+Na]^+$	x	
742.5392	742.56	$[PE(36:2)-H]^-$		x
744.5538	744.55	$[PE(36:2)+H]^+$	x	
745.5025	745.52	$[PG(34:2)-H]^-$		x
747.5176	747.57	$[PG(34:1)-H]^-$		x
754.5363	754.55	$[PE(35:1)+Na]^+$	x	
756.5549	756.58	$[PE(37:2)-H]^-$		x
759.5182	759.58	[PG(35:2-H]$^-$		x
761.5333	761.53	$[PG(35:1)-H]^-$		x
766.5363	766.52	$[PE(36:2)+Na]^+$	x	
773.5338	773.55	$[PG(36:2)-H]^-$		x
787.5495	787.56	$[PG(37:2)-H]^-$		x
1345.9180	1345.90	$[CL(64:3)-H]^-$		x
1347.9337	1347.92	$[CL(64:2)-H]^-$		x
1361.9493	1361.93	$[CL(65:2)-H]^-$		x
1369.9175	1369.92	$[CL(66:5)-H]^-$		x
1373.9505	1373.94	$[CL(66:3)-H]^-$		x
1375.9649	1375.94	$[CL(66:2)-H]^-$		x
1383.9331	1383.93	$[CL(67:5)-H]^-$		x
1387.9649	1387.95	$[CL(67:3)-H]^-$		x
1389.9806	1389.96	$[CL(67:2)-H]^-$		x
1395.9331	1395.92	$[CL(68:6)-H]^-$		x
1397.9487	1397.93	$[CL(68:5)-H]^-$		x
1399.9644	1399.95	$[CL(68:4)-H]^-$		x
1401.9806	1401.94	$[CL(68:3)-H]^-$		x
1409.9487	1409.92	$[CL(69:6)-H]^-$		x
1411.9644	1411.94	$[CL(69:5)-H]^-$		x
1413.9801	1414.00	$[CL(69:4)-H]^-$		x
1415.9957	1416.00	$[CL(69:3)-H]^-$		x
1418.0114	1418.00	$[CL(69:2)-H]^-$		x
1423.9644	1423.94	$[CL(70:6)-H]^-$		x
1425.9801	1425.95	$[CL(70:5)-H]^-$		x
1427.9957	1427.90	$[CL(70:4)-H]^-$		x
1430.0114	1429.99	$[CL(70:3)-H]^-$		x
1439.9957	1439.98	$[CL(71:5)-H]^-$		x
1442.0114	1441.99	$[CL(71:4)-H]^-$		x
1444.0270	1444.00	$[CL(71:3)-H]^-$		x
1454.0114	1453.99	$[CL(72:5)-H]^-$		x
1456.0270	1456.00	$[CL(72:4)-H]^-$		x
1458.0426	1457.99	$[CL(72:3)-H]^-$		x

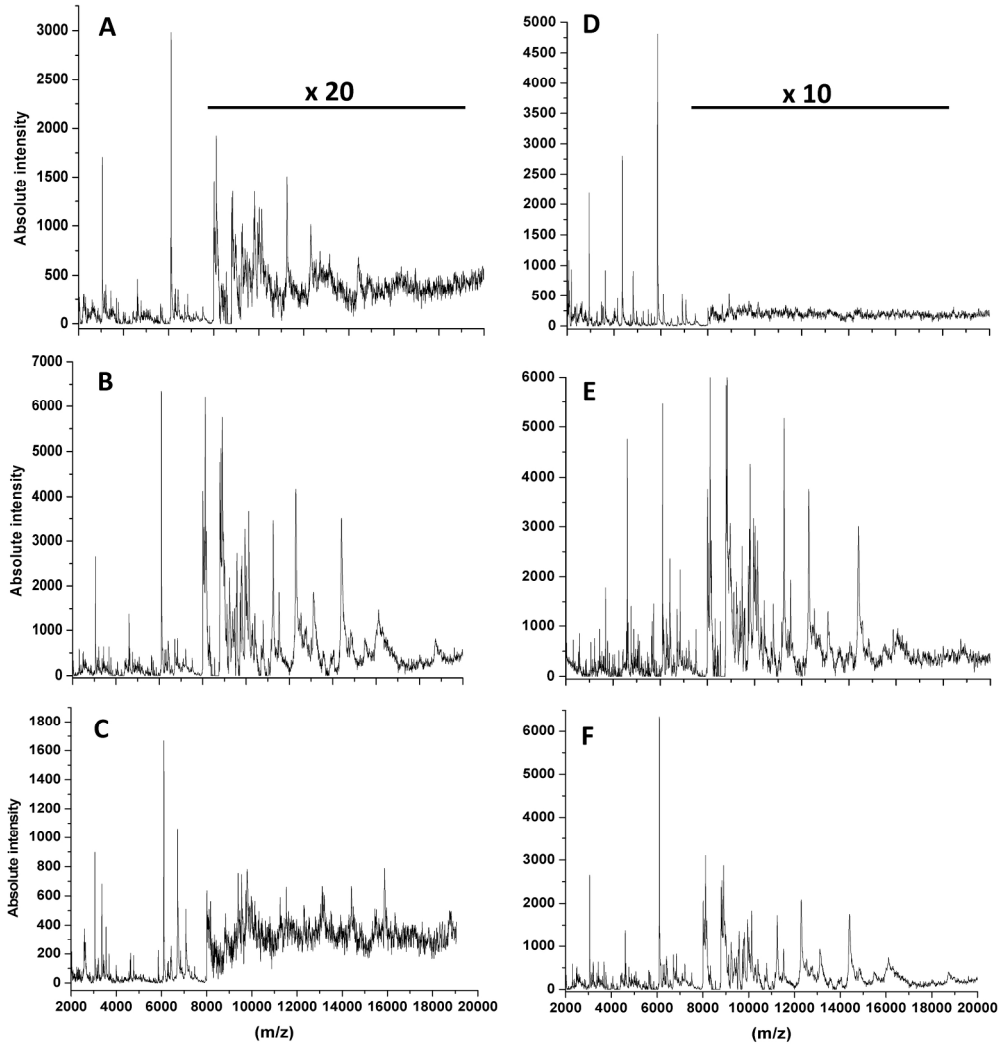

Figure 1

208x224mm (300 x 300 DPI)

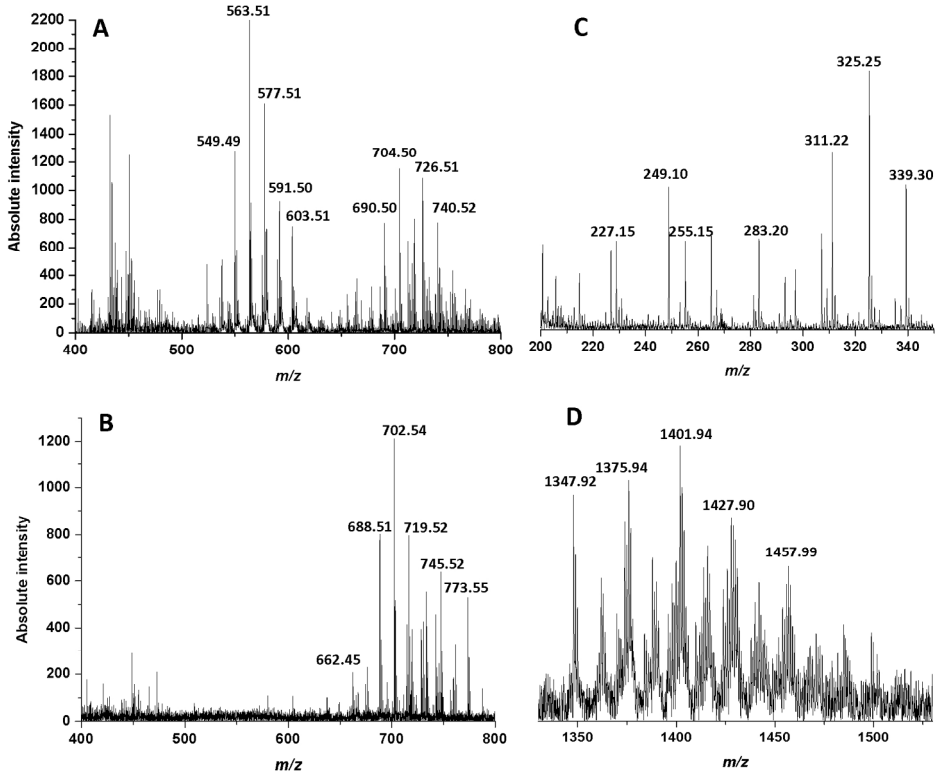

Figure 2

179x161mm (300 x 300 DPI)

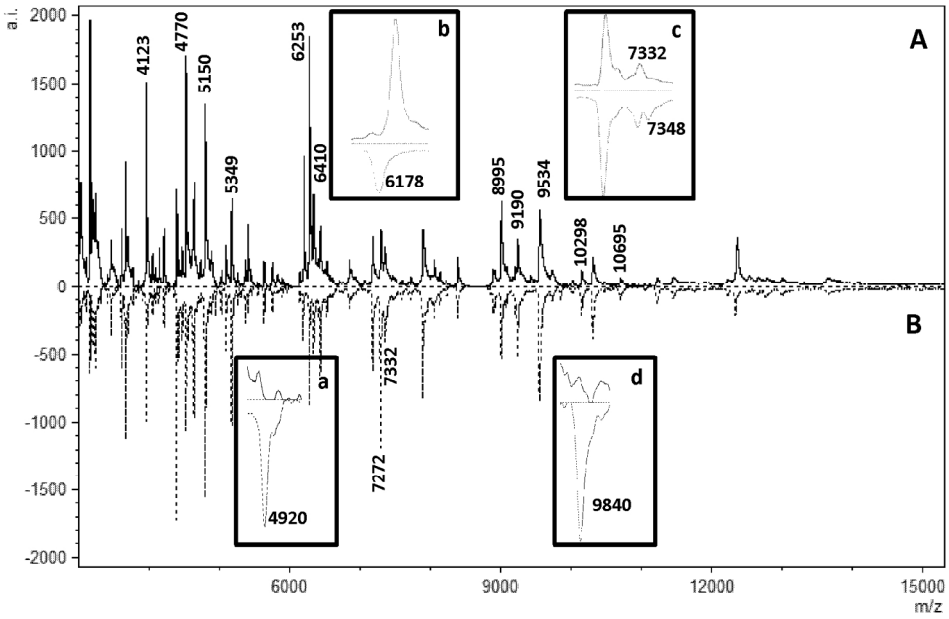

Figure 3

164x110mm (300 x 300 DPI)

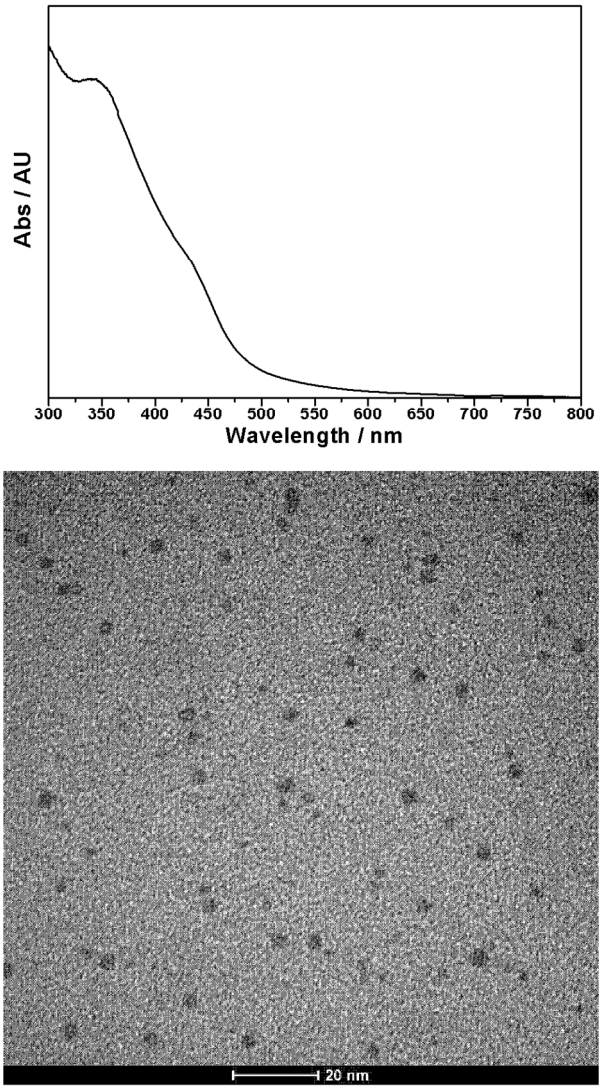

Figure 4

92x165mm (300 x 300 DPI)

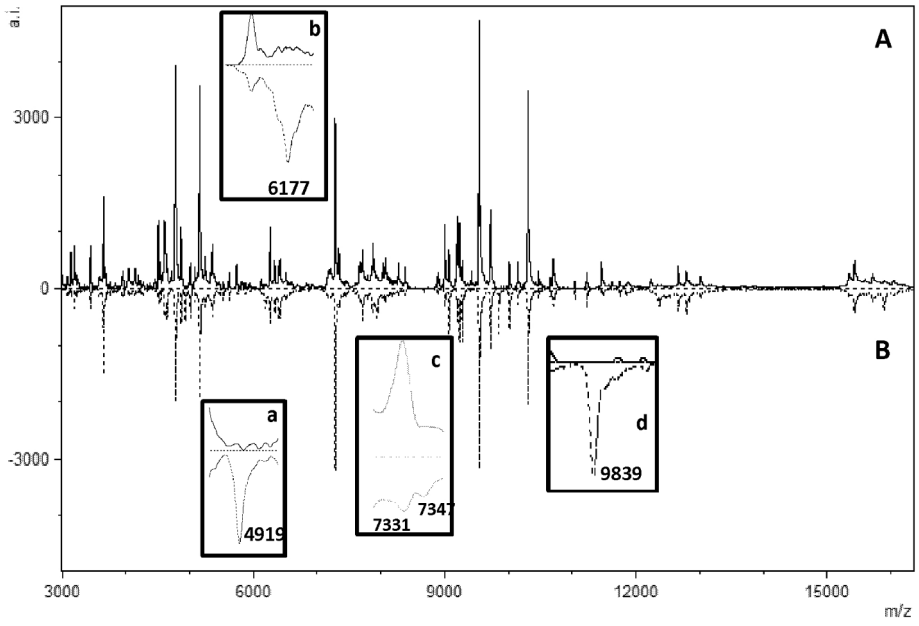

Figure 5

531x389mm (96 x 96 DPI)

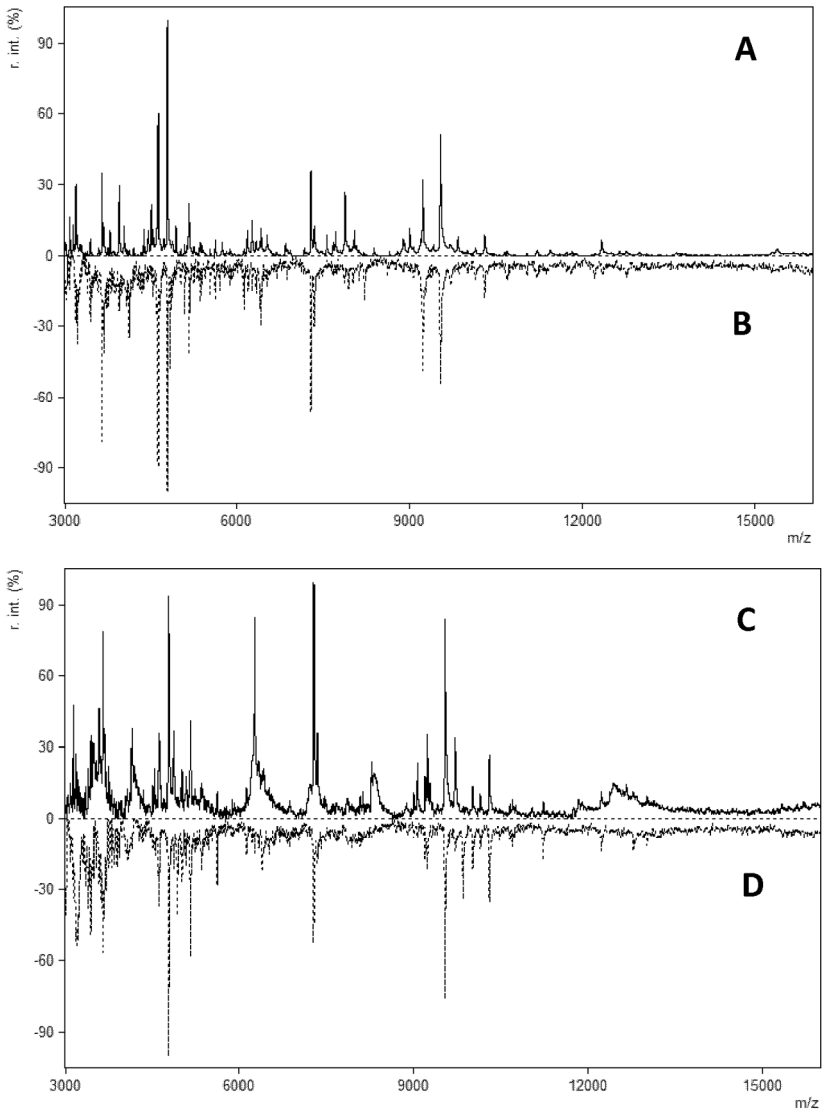

Figure 6

139x183mm (300 x 300 DPI)

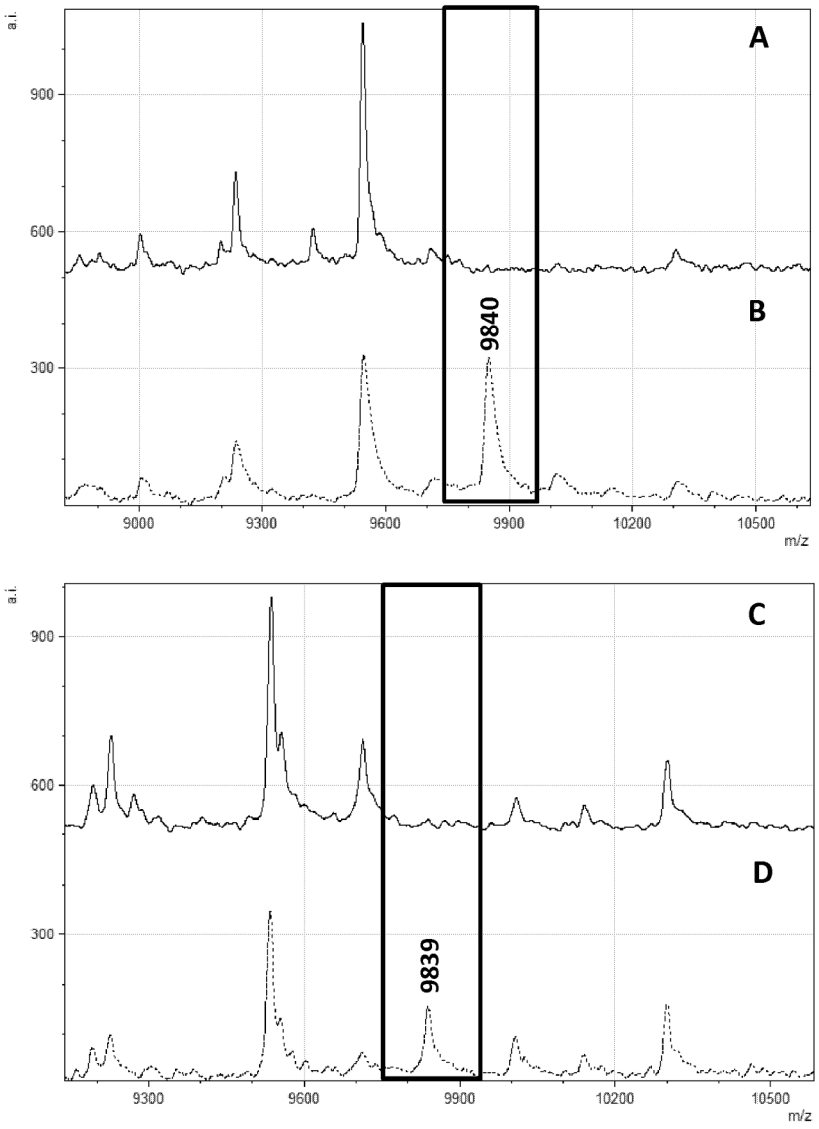

Figure 7

145x201mm (300 x 300 DPI)

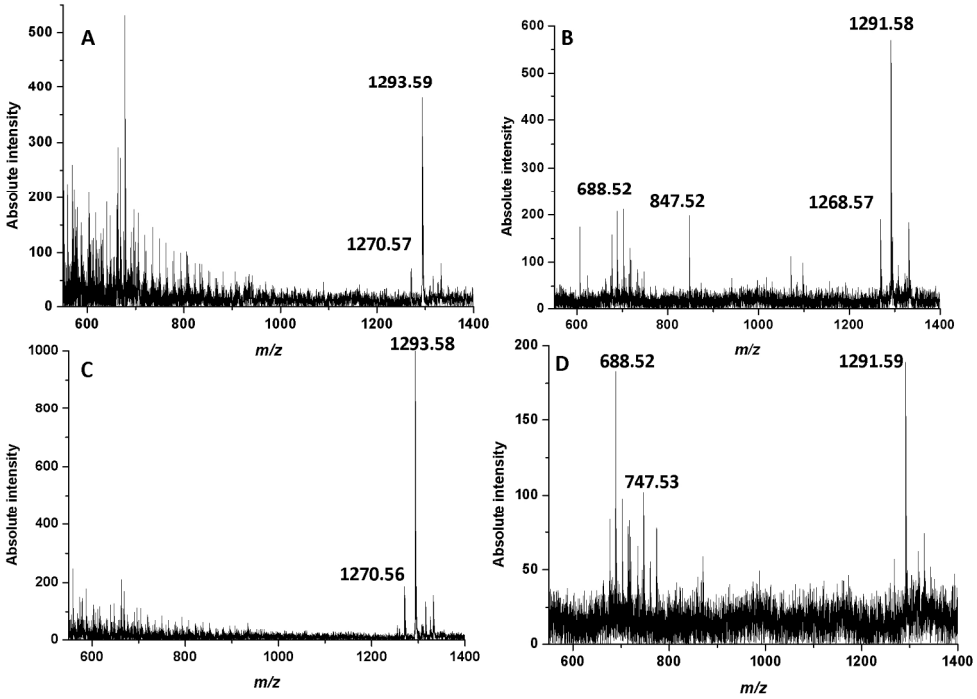

Figure 8

196x147mm (300 x 300 DPI)